# The role of *KCNQ1* in mouse and human gastrointestinal cancers

**B. L. N Than**[1,7], **J. A. C. M. Goos**[2], **A. L. Sarver**[4], **M. G. O'Sullivan**[5], **A. Rod**[1], **T. K. Starr**[3,6], **R. J. A. Fijneman**[2], **G. A. Meijer**[2], **L Zhao**[1], **Y Zhang**[8], **D. A. Largaespada**[3], **P. M. Scott**[1], and **R. T. Cormier**[1,**]

[1]Department of Biomedical Sciences, University of Minnesota Medical School, Duluth, MN 55812
[2]Dept. of Pathology, VU University Medical Center, 1081 HV, Amsterdam, Netherlands
[3]Department of Genetics, Cell Biology & Development, Center for Genome Engineering, Masonic Cancer Center, University of Minnesota, Minneapolis, MN 55455 [4]Department of Biostatistics and Informatics, Masonic Cancer Center, University of Minnesota, Minneapolis, MN 55455 [5]College of Veterinary Medicine, University of Minnesota, St. Paul, MN 55108 [6]Department of Obstetrics, Gynecology & Women's Health, Masonic Cancer Center, University of Minnesota Medical School, Minneapolis, MN 55455 [7]Toxicology Graduate Program, University of Minnesota, Duluth, MN 55812 [8]University of Minnesota Supercomputing Institute, Minneapolis, MN 55455

## Abstract

*Kcnq1,* which encodes for the pore-forming alpha subunit of a voltage-gated potassium channel, was identified as a gastrointestinal (GI) tract cancer susceptibility gene in multiple *Sleeping Beauty* DNA transposon-based forward genetic screens in mice. To confirm that *Kcnq1* has a functional role in GI tract cancer we created *Apc^Min* mice that carried a targeted deletion mutation in *Kcnq1*. Results demonstrated that *Kcnq1* is a tumor suppressor gene as *Kcnq1* mutant mice developed significantly more intestinal tumors, especially in the proximal small intestine and colon, some of these tumors progressed to become aggressive adenocarcinomas. Gross tissue abnormalities were also observed in the rectum, pancreas and stomach. Colon organoid formation was significantly increased in organoids created from *Kcnq1* mutant mice compared with wildtype littermate controls, suggesting a role for *Kcnq1* in regulation of the intestinal crypt stem cell compartment. To identify gene expression changes due to loss of *Kcnq1* we carried out microarray studies in colon and proximal small intestine. We identified altered genes involved in innate immune responses, goblet and Paneth cell function, ion channels, intestinal stem cells, EGFR and other growth regulatory signaling pathways. We also found genes implicated in inflammation and in cellular detoxification. Pathway analysis using Ingenuity Pathway Analysis (IPA) and gene set enrichment analysis (GSEA) confirmed the importance of these gene clusters and further identified significant overlap with genes regulated by *MUC2* and *CFTR*, two important regulators

**corresponding author: Robert T. Cormier, Ph.D., University of Minnesota Medical School, 1035 University Drive, Duluth, MN 55812; Tel# 218-726-8625; Fax# 218-726-8014; rcormier@d.umn.edu.

**Conflict of interest.** The authors state that there are no conflicts of interest to declare.

of intestinal homeostasis. To investigate the role of *KCNQ1* in human colorectal cancer (CRC) we measured protein levels of KCNQ1 by immunohistochemistry in tissue microarrays containing samples from CRC patients with liver metastases who had undergone hepatic resection. Results showed that low expression of KCNQ1 expression was significantly associated with poor overall survival (OS).

## Keywords

colorectal cancer; *KCNQ1*; tumor suppressor

## Introduction

The *KCNQ1* gene encodes for the pore-forming alpha subunit of a voltage-gated potassium channel that enables a K+ current after electrical depolarization of the cell membrane. *KCNQ1* is predominantly expressed in myocardium, inner ear, stomach, intestine and pancreas, tissues in which *KCNQ1* expression is critical for ion homeostasis[1]. Inherited mutations in *KCNQ1* underlie several human disease syndromes. For example, mutations in *KCNQ1* are associated with congenital *long QT syndrome* (LQTS), a disorder caused by abnormal ventricular repolarization that increases the risk of sudden death from cardiac arrhythmias. *Jervell and Lange-Nielson syndrome* (JLNS) is a rare autosomal disorder characterized by deafness in addition to LQTS. Recent reports indicate that JLNS patients can also be susceptible to gastrointestinal defects including iron-deficiency anemia, gastric and duodenal hyperplasia, elevated gastrin levels, and more rarely, gastric adenocarcinoma[2–5]. Variants in KCNQ1 are also associated with enhanced risk for type-2 diabetes[6,7].

Relatively little is known about the role of *KCNQ1* in cancer, but a potential role in gastrointestinal (GI) tract cancers was indicated by its identification as a high frequency common insertion site (CIS) locus in *Sleeping Beauty* (*SB*) DNA transposon-based forward mutagenesis genetic screens for intestinal[8,9] and pancreatic cancer[10,11]. In our forward genetic screen in *Apc* wildtype mice we found *Kcnq1* mutations in 18 intestinal tumors (13%)[8], ranking it among the top 10 CIS genes. In this study, while transposon insertions in *Kcnq1* were found in tumors from all regions of the intestine, approximately 2/3 (64%) were located in the duodenum and jejunum, with 26% in the ileum and 10% in the colon. Furthermore, transposon insertions in *Kcnq1* were observed about equally in both the forward and reverse strand orientation, consistent with a model whereby the transposon is acting to disrupt gene function. We performed a second forward genetic screen in *Apc*[Min] mice and found *Kcnq1* transposon insertions in 13 intestinal tumors (14%)[12]. Another screen in *Apc*[Min] mice found *Kcnq1* transposon mutations in 120 intestinal tumors (27%), ranking it #15 out of 641 CIS genes (120 kb window)[9]. We have also conducted a screen using *p53*[R270H] mutant mice and identified insertions in *Kcnq1* in 15 intestinal tumors (23%) (TKS, *manuscript in preparation*).

Six mutant mouse alleles of *Kcnq1* have been created that partially model human disorders arising from inherited mutations in *KCNQ1*, especially JLNS[13–17]. These mutant alleles

share similar but not identical phenotypes, including bilateral deafness from birth, gastric hyperplasia, gastric achlorhydria, elevated serum gastrin, headbobbing, bi-directional circling, ataxia, body tremor, and hyperactivity with a consequent significant decrease in body weight. Conflicting results were reported regarding a cardiac phenotype in these models. In mouse small intestine, *Kcnq1* expression is strongest in the duodenum and proximal jejunum and decreases towards the ileum[18,19]. In the large intestine *Kcnq1* expression is strongest in distal colon[20,21].

To further investigate the role of *Kcnq1* in GI tract cancers we measured GI cancer phenotypes following introgression of a targeted knockout allele of *Kcnq1*[14] into the *Apc^Min* model of intestinal tumorigenesis. We then investigated the role of *KCNQ1* in progression of human colorectal cancer (CRC) by measuring KCNQ1 protein levels in tissue microarrays containing samples from more than 500 CRC patients with liver metastases. Results from both of these studies indicate that *Kcnq1* is a tumor suppressor.

## Results

### Loss of *Kcnq1* enhances tumor multiplicity in *Apc^Min* mice

Haploinsufficiency for *Kcnq1* significantly enhanced *Apc^Min* intestinal tumor multiplicity overall, in both males and females, by ~ 40% (Table 1), with the phenotype strongest in the proximal small intestine and colon, where tumors increased ~ 2-fold. *Kcnq1^{−/−}* mice in our study manifested a range of previously reported phenotypes: rapid bi-directional circling, ataxia, tremor, head bobbing, and they were smaller (~↓25%, body weight) and leaner than littermate *Kcnq1* wildtype and heterozygous mice. Less than half of the expected number of *Apc^Min* *Kcnq1^{−/−}* mice survived until weaning (23 *vs* ~ 60). Survivor *Apc^Min* *Kcnq1^{/−}* mice demonstrated a very strong increase in tumors in the proximal half of the small intestine (~3-fold), especially in the proximal quarter of the small intestine containing the duodenum and proximal jejunum (Table 2), the region exhibiting strongest expression of *Kcnq1* in the intestine. *Apc^Min* *Kcnq1^{−/−}* mice developed ~ 2-fold increase in colon tumors but no increase in the distal small intestine of males, and a decrease in females. No significant differences between *Kcnq1* genotypes in tumor sizes were observed.

### Loss of *Kcnq1* promotes tumor progression

Tumors in *Apc^Min* mice are invariably benign adenomas that usually vary in size between 0.3 mm to ~5 mm. Adenocarcinomas are extremely rare. In *Apc^Min* mice carrying either heterozygous or homozygous mutations in *Kcnq1* development of adenocarcinomas occurred at a frequency of ~10–15%. These adenocarcinomas appeared as large lesions (some greater than 20 mm), located in the proximal small intestine in a region approximate with the duodenal jejunal flexure at the head of the pancreas. In almost all cases there was buckling of the intestinal tube, in two cases there was a pronounced intussusception of the tissue and in two cases the tumors extended across the entire inner surface of the intestinal lumen. Six of these large tumors were analyzed by histopathology and all were found to be invasive adenocarcinomas (Fig. 1). Fig. 1A depicts a lesion of > 2 cm in length from the duodenum of an *Apc^Min* *Kcnq1^{+/−}* mouse, that when sectioned regionally, revealed adenocarcinoma tissue in each section. No adenocarcinomas were detected in the remainder

of the small intestine or in the large intestine, and no putative adenocarcinomas were detected in $Apc^{Min}$-$Kcnq1^{+/+}$ mice.

### Loss of *Kcnq1* is associated with other pathologies in the GI tract

Rectal prolapse was evident in ~ 10% of $Apc^{Min}$ $Kcnq1^{+/-}$ and $Apc^{Min}$ $Kcnq1^{-/-}$ mice and in several cases the rectal prolapses were associated with enlarged rectums characterized by diffuse severe crypt hyperplasia (Supp. Fig. 1). In addition, $Kcnq1^{-/-}$ mice developed severe gastric hyperplasia that was characterized by mucosal hyperplasia, with parietal cells increased in size and crypt dilation with extensive cellular debris (Supp. Fig. 2). Hyperplastic adenomas in the pylorus were also present in $Apc^{Min}$ $Kcnq1$ mutant mice. While $Apc^{Min}$ $Kcnq1^{+/-}$ mice showed an incidence of pyloric tumors of ~ 30%, the phenotype was much stronger in $Apc^{Min}$ $Kcnq1^{-/-}$ mice where the incidence of pyloric tumors was greater than 90% (21/23). Furthermore, in $Apc^{Min}$ $Kcnq1^{-/-}$ mice pyloric tumor multiplicity was much larger, with some mice developing as many as a dozen tumors. No pyloric tumors were observed in $Apc^{Min}$ $Kcnq1^{+/+}$ mice. Finally, roughly one third of $Apc^{Min}$ $Kcnq1^{-/-}$ mice developed grossly and severely enlarged (~2–3 fold) pancreases, characterized by extra lobes. Histopathology of a matched pair of samples indicated that zymogen granules were less eosinophilic and less prominent, and that both exocrine cells and islets were smaller (Supp. Fig. 3).

### Loss of *Kcnq1* has a strong effect on gene expression

We conducted cDNA microarray expression studies using tissue from distal colon and the proximal quarter of the small intestine of $Apc^{+/+}$ $Kcnq1^{-/-}$ mice. Overall, more than 400 genes showed a greater than 1.5 fold change in expression, and greater than 200 of these genes also had a P value of < 0.05 (Supp. Tables 1&2). Expression of 20 genes was confirmed by RT-PCR (Figures 2 & 3). Target genes were clustered into several functional groups: innate immune response/goblet & Paneth cell function (*Ang4, Retnlb, Clps, Pnliprp2, Clca3, Muc2, Reg3a, Reg3b, Reg3g, Car1*), ion channels (*Trpv6, Slc12a8, Slc30a10, Aqp7, Aqp1, Aqp8, Aqp4, Clca3, Clca6*), mucins (*Muc2, Muc13, Muc4, Muc3*), growth regulatory signaling pathways (*Areg, Egr1, Fos, Ccdn1*), cancer cell migration (*Mmp9, Mmp15, S100a14, Mt1*), apoptosis (*Casp14, Casp2, Bcl6*), inflammation, mediated by mechanisms such as detoxification & stress responses (*Cyp2c55, Gstk1, Sirt1, Sirt3, Aldh1a1, Aldh1b1, Aldh2, Mt1, Gstm2*), the adaptive immune response, and intestinal stem cell-related genes (*Clca4, Aqp4, Aldh1a1, Olfm4*), consistent with a role for *Kcnq1* in the intestinal cell compartment[22]. Interestingly, while loss of *Kcnq1* showed a strong effect on colon secretory cell genes, there was no change in colon tissues in the secretory cell populations or cell proliferation (Supp. Fig. 4).

### *Kcnq1, Cftr* and *Muc2* share common genetic pathways in the GI tract

IPA analysis[23] identified significant networks and functional groups altered in *Kcnq1* KO mice. See Supp. Fig. 5A & 5B and Supp. Table 3, colon; and Supp. Fig. 6 and Supp. Table 4, proximal small intestine. In particular, IPA analysis identified *Cftr* as a top upstream regulator of *Kcnq1* KO dysregulated genes indicating that genes differentially expressed in the *Kcnq1* KO mice overlap with targets of *Cftr* (overlap p-value of 5.81E-13, activation Z-

score −2.722). Furthermore, the *Cftr* network is predicted to be down regulated in *Kcnq1* KO small intestine suggesting that *Kcnq1* may be necessary for some aspects of *Cftr* function.

To identify common pathways and genes disrupted by *Kcnq1* and *Cftr* deficiencies we used Gene Set Enrichment Analysis (GSEA)[24]. The entire ranked expression data set from the *Kcnq1* KO proximal small intestine array was compared to genesets compiled from a microarray analysis of gene expression in the small intestine of *Cftr* KO mice[25]. *Cftr* genesets consisted of all genes up or down regulated by 2-fold in the *Cftr* KO mouse. GSEA revealed significant correlation, with overlap of gene identity and direction of regulation. (Fig. 4 and Supp. Table 5, normalized enrichment score (NES) for *Cftr* KO upregulated genes 1.97, $p < 0.001$; NES for *Cftr* KO downregulated genes −1.92, $p < 0.001$.)

These shared targets included a large subset of genes involved in lipid metabolism and, in particular, downregulation of genes involved in lipid oxidation. In support of the significance of this overlap, IPA analyses of *Kcnq1* KO and *Cftr* KO mice each identified lipid metabolism as a major functional category, with oxidation of lipids as the subcategory showing the most significant down regulation (*Kcnq1*, p-value 9.78E-06, activation z-score, −2.26; *Cftr*, p-value 9.37E-09, z-score, −3.62). Common targets included upregulation of *Idi1*, involved in cholesterol synthesis, and downregulation of *Hsd174b* and *Acaa1b*, both involved in fatty acid beta oxidation. Inhibition of fatty acid oxidation is associated with a switch to lipogenesis and this switch is characteristic of metabolic remodeling that commonly occurs during oncogenesis[26]. Also, fatty acid metabolism has recently been shown to play a key role in stem cell maintenance with lipogenesis associated with more highly proliferating stem cells[27]. Thus, altered lipid metabolism may contribute to development of CRC in *Kcnq1* and *Cftr* KO mice.

A second group of genes dysregulated in both *Kcnq1* KO mice and *Cftr* KO mice is involved in inflammation. Because the intestinal epithelium is constantly exposed to flora and foreign substances it must maintain protective and repair mechanisms. Disruption of these protective or homeostatic processes can result in inflammatory changes, which in turn are associated with inflammatory bowel disease and increased risk of CRC[28]. Genes involved in inflammation are dysregulated in both *Kcnq1* KO mice and *Cftr* KO mice. These include upregulation of factors normally produced by intestinal epithelial cells to maintain immune homeostasis including Il7[29], Reg3g[30] and Pglryp1[31]. In addition, a number of protective genes are down regulated including those involved in detoxification, *Gstt1*, *Cyp3a11*, *Cyp2b10*, and others involved in protective signaling, such as *Sema7a*, which promotes Il10 signaling[32], and *Ace2* which protects against inflammation-induced epithelial damage[33]. Further evidence of overlap between KCNQ1 and CFTR was provided by analyzing RNA Seq data from 20 CRC liver metastases samples for concordance between expression levels of each gene. Using Pearson's Correlation analysis of FPKM values in the 20 samples it was found that *KCNQ1* and *CFTR* were significantly co-expressed, despite up to a 10-fold sample-to-sample FPKM variability for each gene. See Supp. Figs. 7A, 7B. Finally, both *KCNQ1* and *CFTR* are regulated downstream of the serine threonine kinase gene *SGK1*, which is activated by factors including insulin, via the PI3K pathway, under conditions of osmotic stress[34]. *SGK1* levels in turn appear to be influenced by the activity of

both *KCNQ1* and *CFTR*, as *Sgk1* expression was up-regulated by more than 2-fold in *Kcnq1* KO colon (Supp. Table 1) and was also up-regulated by > 1.6-fold in *Cftr* KO colon (BLNT, *manuscript in preparation*). Of further interest, *Sgk1* expression levels were down-regulated by 1.5-fold in the proximal small intestine of *Kcnq1* KO mice and down-regulated by 5.5-fold in the small intestine of *Cftr* KO mice[25].

CFTR export of Cl- and HCO3- maintains extracellular $H_2O$ homeostasis, which in turn is necessary for hydration and function of the protective lumenal mucin layer[35]. Another gene directly involved in maintenance of the mucin layer is *MUC2*, which encodes MUCIN2, one of the major glycoproteins making up this layer. As with *Kcnq1* and *Cftr, Muc2* deficiency is implicated in CRC[36]. To test if common pathways were disrupted by loss of *Kcnq1* and *Muc2*, we compared gene expression changes in the *Kcnq1* KO mouse with those reported for *Muc2* KO mice[36]. GSEA identified significant overlap in gene expression with genes down regulated in *Muc2* KO mice enriched in genes down regulated in *Kcnq1* KO mice. (Fig. 4 and Supp. Table 5, NES −1.80, p < 0.001.) This group included a number of genes involved in detoxification including cytochrome oxidase p450 enzymes and several glutathione S-transferases, *Gsta2, Gstm2, Gstm4, Gstm6,* and *Gstt1*. Moreover, in a separate study[37], deficiency for *Muc2* in the mouse intestine resulted in significant increases in the innate immune responders *Reg3g* and *Reg3b*, matching our findings in *Kcnq1* KO mice. Finally, we found that *Areg*, an EGFR pathway gene that was upregulated in both the colon and proximal small intestine of *Kcnq1* KO mice, was also upregulated by > 10 fold in the colon of *Muc2* KO mice (RTC & RJAF, *unpublished microarray results*) and in the colon of *Cftr* KO mice (BLNT, *manuscript in preparation*). See Supp. Table 6.

### Loss of *Kcnq1* promotes colon organoid development

To investigate a role for *Kcnq1* in the intestinal stem cell compartment we created intestinal organoids from the colons of a group of *Kcnq1^{+/+}* and *Kcnq1^{−/−}* age and gender matched littermate mice. At days 2 through 5, organoid growth was monitored and organoid number counted on day 5. Loss of *Kcnq1* increased the number of colon organoids by greater than 3-fold, confirming a potential regulatory effect of *Kcnq1* on the intestinal stem cell compartment[22] (Fig. 5).

### KCNQ1 expression is associated with good prognosis in late stage human CRC

Based on our finding that deficiency for *Kcnq1* drove the progression of intestinal tumors in mice we tested the hypothesis that low levels of KCNQ1 in human CRC would correlate with a worse prognosis. To this end, we evaluated KCNQ1 protein expression in tissue microarrays containing samples from more than 500 stage IV CRC patients with liver metastases who had undergone hepatic resection. Immunohistochemical staining for KCNQ1 expression was evaluated for 311 patients. Membranes of neoplastic CRC liver metastasis (CRCLM) epithelium were scored for KCNQ1 staining intensity (Fig. 6). We found that high KCNQ1 expression was related to improved overall survival (OS) (HRR 0.64; 95%CI 0.45–0.92; *P*=.02). Median OS for patients with high KCNQ1 expression was 60 months, while patients with low KCNQ1 levels had a median OS of 37 months, indicating a significant *23-month difference* in survival (Fig. 7).

Next, we performed a multivariate analysis to evaluate whether the prognostic value of KCNQ1 protein expression was independent of established prognostic clinicopathological variables, i.e., primary tumor-to-liver metastasis interval > 12 months, number of liver metastases > 1, maximal tumor diameter > 5.0 cm, lymph node positivity at time of diagnosis of the primary tumor and serum CEA level > 200 ng/ml. Upon stepwise backward Cox regression analysis with OS as the dependent variable, KCNQ1 expression (HRR 0.49; 95%CI 0.32–0.77; *P*=.002), lymph node positivity at time of diagnosis of the primary tumor (HRR 1.64; 95%CI 1.08–2.48; *P*=.02) and maximal tumor diameter > 5.0 cm (HRR 1.44; 95%CI 0.96–2.16; *P*=.08) were retained as prognostic variables. Note that the association between maximal tumor diameter and survival was not significant, however, the variable was retained in the model because we only excluded variables when *P*>0.1.

## Discussion

We first identified *Kcnq1* as a potential CRC driver gene in our forward genetic screens for GI tract cancer genes. Here, we have followed up with studies using a transgenic mouse model and analysis of human CRC tissues that support a tumor suppressor role for *Kcnq1*. We demonstrated the tumor suppressor function of *Kcnq1* in *Apc^Min^* mice, where both hetero- and homozygous inactivation of *Kcnq1* resulted in significantly more adenomas and, importantly, progression to adenocarcinoma. This was especially evident in the proximal small intestine. Furthermore, *Kcnq1* deficiency caused rectal adenomatous hyperplasia, pyloric tumorigenesis, gastric hyperplasia, and pancreatic abnormalities.

Notably, in human CRC that had metastasized to the liver, low KCNQ1 protein expression correlated with significantly lower OS, by almost 2 years, compared to patients with high KCNQ1 expression. These findings suggest that KCNQ1 expression could be a biomarker to help determine eligibility for hepatic resection in CRC patients with liver metastases. In addition, newly developed small molecules that enhance K+ ion channel activity[38,39] could potentially be used to treat CRC patients with low levels of KCNQ1.

By what mechanism does loss of *KCNQ1* influence cancer processes in the GI tract? A promising model is via *KCNQ1*'s functional interactions with *CFTR* and *MUC2*. In the healthy intestinal epithelium KCNQ1 is physiologically linked to the CFTR ion channel, with basolateral export of K+ ions by KCNQ1 providing the electrochemical driving force for apical export of Cl- ions by CFTR[40]. *Cftr* was identified as a CRC driver gene in two SB GI tract forward genetic screens[8,9], and individuals with cystic fibrosis, caused by inactivating mutations in *CFTR*, are at increased risk for GI cancers including CRC[41]. To test if common pathways and genes are disrupted by loss of *Kcnq1* and *Cftr* activity we used GSEA to compare genesets consisting of genes reported to be up or down-regulated in the small intestine of *Cftr* KO mice to the entire ranked *Kcnq1* expression dataset and found significant correlation (Fig. 4). Genes upregulated in common include several involved in immune responses and inflammation, while genes downregulated in common include a subset involved in fatty acid metabolism, in particular lipid oxidation. Further evidence of overlap between *KCNQ1* and *CFTR* was the finding of concordance between *KCNQ1* and *CFTR* expression in RNA Seq analysis of twenty CRC liver metastases (Supp. Figs. 7A, 7B).

As with *Kcnq1* and *Cftr, Muc2* deficiency is implicated in CRC[36]. To test if common pathways were disrupted by loss of *Kcnq1* and *Muc2*, we compared gene expression changes in the *Kcnq1* KO mice with those reported for *Muc2* KO mice[27]. GSEA identified significant overlap in gene expression with genes down regulated in *Muc2* KO mice enriched in genes down regulated in *Kcnq1* KO mice (Fig. 4). This group included a number of genes involved in detoxification including cytochrome oxidase p450 enzymes and several glutathione S transferases, and genes involved inflammation.

These results point to common pathways (inflammation, lipid metabolism, detoxification and stress responses) disrupted by *Kcnq1, Cftr* and *Muc2* deficiencies. Therefore we can hypothesize that *KCNQ1*, like *MUC2* and *CFTR,* may act through one or more of these pathways in preventing cancer in the GI tract. Moreover, precisely defining mechanisms of action for *KCNQ1* can lead to its use as a prognostic predictor for CRC patients and potential therapeutic target.

## Materials and Methods

### Mice

C57BL/6J mice and C57BL/6J-*Apc^Min* mice were obtained from the Jackson Laboratory (Bar Harbor, ME). C57BL/6-*Kncq1* knockout mice were obtained from Dr. Karl Pfeifer (NIH)[14]. Details of mouse husbandry are as previously described[43]. The genotype of the *Apc and Kcnq1* loci were determined by PCR assays as previously described[14,42].

### Tumor analysis

Scoring of GI tumor tissues was performed as previously described[42]. Two-sided P values for tumor counts were determined by use of the Wilcoxon Rank Sum Test comparing gender and age-matched classes produced in the same genetic crosses.

### Histopathology

Histopathological analysis of tumors and adjoining normal tissue was performed on FFPE tissues by an A.C.V.P.-certified veterinary pathologist (M.G.O'S.) from the University of Minnesota Masonic Cancer Comparative Pathology Shared Resources facility using protocols as previously described[42].

### Organoid Culture

Gender, age, and littermate-matched C57Bl/6J *Kcnq1^{+/+}* and *Kcnq1^{−/−}* mice were sacrificed between 8 and 12 weeks of age. Colons were removed, cut open and washed in cold PBS. Colon organoids were then cultured using the protocol of Sato et al, 2011[43], following the plating of 500 crypt bottoms per well in triplicate per sample.

### RNA processing for Illumina Bead Arrays

Mouse intestinal tissues were removed, opened longitudinally, and rinsed in PBS. Colon tissues were processed in RNAlater (Qiagen) per manufacturer's protocol. The distal quarter of the proximal quarter of the small intestine was flash frozen in liquid nitrogen. Tissue was then transferred from liquid nitrogen to pre-cooled RNALaterIce (Ambion) at −80°C for

30min, and then was transferred to −20°C for at least 48hrs. Immediately before RNA isolation, tissue in either RNALater or RNALaterIce was placed in 2–4 mL of RLT/14.3M β-mercaptoethanol (BME) buffer. Tissue was then homogenized using an IKA Ultra-Turrax T25 digital homogenizer (Fisher Scientific). RNA isolation was then conducted using an RNeasy Mini Kit with an additional DNAse Digestion step (Qiagen). RNA sample concentrations were measured using a Nanodrop-1000 Spectrophotometer (Thermo Scientific). RNA was stored at −80°C.

### Illumina Bead Microarray and Data Analysis

RNA labeling, microarray hybridization and scanning were performed at the University of Minnesota – BioMedical Genomics Center using Illumina MouseWG-6 v2.0 Expression BeadChips (Illumina, San Diego, CA, USA), according to the manufacturer's instructions. Differential expression of genes was quantified by the moderated t-statistic. Data were analyzed using GeneData Expressionist Software (GeneData Inc, San Francisco, CA); genes that showed statistically significant differences in expression between groups were determined using the two-group *t*-test and ANOVA. Gene expression data has been submitted to the Gene Expression Omnibus (GEO), Accession number pending.

### qRT-PCR

Quantitative RT-PCR was performed as previously described[17]. Significant differences in expression between groups were determined using the two-group *t*-test.

### List of primers used

All primers were designed using Primer-BLAST (National Center for Biotechnology Information) and obtained from Integrated DNA Technologies.

## Mouse Primers

**Ang4:** Forward = 5′-AGCACACAGCTAGACTCGTCCC-3′; Reverse = 5′-ACCAGACCCAGCACGAAGACC-3′

**Areg:** Forward = 5′-GGTCTTAGGCTCAGGCCATTA-3′; Reverse = 5′-CGCTTATGGTGGAAACCTCTC-3′

**Cd55:** Forward = 5′-GGGGCTATGATCCGTGGGCG-3′; Reverse = 5′-TGCCCAAGATTGGCCTGGCA-3′

**Clca3:** Forward = 5′-CCACACCAAAACGAGAAGGC-3′; Reverse = 5′-TGCTTCGGAGATTGCATCGT-3′

**Clca4:** Forward = 5′-ACATGGACCGGCCTTTCTAC-3′; Reverse = 5′-CGACATCTCCTCGACACACA-3′

**Clca6:** Forward = 5′-GTTCAATCAGAAAAGGCTTCCA-3′; Reverse = 5′-ACTTCCCAAGTGCTTCTGTAATTG-3′

**Gstk1:** Forward = 5′-TGGATGCGTGTATGGTCTCG-3′; Reverse = 5′-CAGAAAGTGTTGGGCTTGCG-3′

**Egr1:** Forward = 5′-CCTCAAGGGGAGCCGAGCG-3′; Reverse = 5′-AACCGAGTCGTTTGGCTGGG-3′

**Fos:** Forward = 5′-CGGGTTTCAACGCCGACTA-3′; Reverse = 5′-TTGGCACTAGAGACGGACAGA-3′

**Id1:** Forward = 5′-CTCAGCACCCTGAACGGCGA-3′; Reverse = 5′-CATCTGGTCCCTCAGTGCGCC-3′

**Muc2:** Forward = 5′-AACGATGCCTACACCAAGGTC-3′; Reverse = 5′-ACTGAACTGTATGCCTTCCTCA-3′

**Muc3:** Forward = 5′-CACTACCACCCCAGCACCTA-3′; Reverse = 5′-GCCTCCATTCTCGCAGTTGA-3′

**Muc13:** Forward = 5′-TTTGGCTACAGCGGGATGAA-3′; Reverse = 5′-TCTTTGACCTCGCAGAGACG-3′

**Mt1:** Forward = 5′-AAACCCTTTGCGCCCGGACT-3′; Reverse = 5′-AGCAGGAGCAGTTGGGGTCC-3′

**Pim3:** Forward = 5′-GCTCATCGACTTCGGCTCGGG-3′; Reverse = 5′-AGTGGCAGACCGCCCGTGATA-3′

**Retnlb:** Forward = 5′-AAGCCTACACTGTGTTTCCTTTT-3′; Reverse = 5′-GCTTCCTTGATCCTTTGATCCAC-3′

## Pathway Analysis

**Gene Set Enrichment Analysis (GSEA)—**GSEA v2.0, http://www.broad.mit.edu/gsea/[24,44]. Gene sets analyzed were obtained from published reports and the NCBI GEO database.. GSEA compared the entire ranked *Kcnq1* proximal SI KO expression data set to *Cftr* KO[25] (2 fold change in expression, t <= 0.05) and *Muc2* KO[36] (1.5-fold change in the duodenum at three or six months of age).

**Ingenuity Pathway Analysis (IPA)—**Genes showing a 1.5 fold change in expression in whole colon (N=89) and proximal small intestine (N=345) microarrays were analyzed using IPA[23].

## Tissue microarrays

**Patient study population—**Patients who underwent liver resection with curative intent, sometimes with addition of RFA, in one of the seven Dutch hospitals affiliated with the DeCoDe PET group were identified by cross-referencing surgery and pathology databases using Dutch MeSH terms for "colon", "rectum", "carcinoma", "adenocarcinoma", "colorectal neoplasms", "liver", "neoplasm metastasis", and "(hemi)hepatectomy". Clinicopathological data from 507 patients that were operated on between 1990 and 2010 were extracted from these databases. See Supp. Table 7 (a manuscript describing the patient population in more detail is *in preparation*). Formalin-fixed paraffin-embedded (FFPE) tissue specimens were collected from one CRCLM sample and an adjacent control liver sample. Only specimens of patients with histologically confirmed CRCLM were included in

the study, while tissue samples of patients with multiple primary tumors were excluded. Collection, storage and use of clinicopathological data and tissue specimens were performed in compliance with the "Code for Proper Secondary Use of Human Tissue in The Netherlands", and approved in protocol 2011–03 of the Department of Pathology[45].

**Tissue microarrays**—A total of 21 TMAs were generated as described previously[46,47]. In brief, three tissue core biopsies of 0.6mm in diameter were punched from morphologically representative areas of all FFPE donor blocks, and transferred into TMA recipient paraffin blocks using the 3DHISTECH TMA Master (v1.14, 3DHISTECH Ltd., Budapest, Hungary).

**Immunohistochemistry**—Four μm sections of TMAs were mounted on glass slides, deparaffinized by xylene and rehydrated with a decreasing alcohol series. Staining for KCNQ1 was performed upon antigen retrieval by microwave heating in citric acid (10 mM, pH6.0) and endogenous peroxidase neutralization in 0.3% hydrogen peroxide in methanol for 25 minutes. The primary rabbit polyclonal antibody directed against human KCNQ1 (sc-20816, Santa Cruz Biotechnology, Inc., Santa Cruz, USA) was incubated overnight at a 1:200 dilution at 4°C, followed by incubation with anti-rabbit secondary antibodies for 30 minutes at room temperature (Envision Plus, Dako, Heverlee, Belgium). Secondary antibodies were visualized by liquid diaminobenzidine (DAB) substrate chromogen system. Slides were counterstained with Mayer's haematoxylin. Staining of FFPE colon tissue was used as a positive control, and incubation without primary antibody as a negative control.

**Evaluation of KCNQ1 protein expression**—Immunohistochemical stainings were digitally captured using the Mirax slide scanner system equipped with a 20x objective with a numerical aperture of 0.75 (Carl Zeiss B.V., Sliedrecht, The Netherlands) and a Sony DFW-X710 Fire Wire 1/3″ type progressive SCAN IT CCD (pixel size 4.65×4.65μm). Actual scan resolution at 20x was 0.23μm. Computer monitors were calibrated using Spyder2PRO software (v1.0-16, Pantone Colorvision, Regensdorf, Switzerland). TMA core biopsies were scored for intensity of KCNQ1 protein expression on membranes of neoplastic epithelial cells (categories negative, weak, moderate, strong) using dedicated TMA scoring software (v1.14.25.1, 3DHISTECH Ltd., Budapest, Hungary). For facilitating scoring a chart with visual analogue scales of staining patterns was used. Intensity scores were dichotomized into low and high KCNQ1 intensities using Receiver Operating Characteristic curve analysis[48].

**Statistical analysis of TMAs**—Overall survival (OS) was defined as the time in months after surgery until death in a follow-up period of 10 years. Patients were excluded from analysis if OS < 2 months (n=72), if OS or survival status were unknown (n=36), or if tissue cores could not be evaluated for technical reasons (n=88). The relation between KCNQ1 expression and survival was studied using Kaplan Meier curves and tested using logrank statistics. Hazard rate ratio (HRR) was calculated using Cox regression. Multivariate analysis was performed by inclusion of KCNQ1 protein expression in a proportional hazards (Cox regression) analysis together with established prognostic clinicopathological variables combined in the clinical risk score as defined by Fong *et al.*[49], primary tumor-to-liver metastasis interval > 12 months, number of liver metastases > 1, maximal tumor diameter >

Author Manuscript

5.0 cm, lymph node positivity at time of diagnosis of the primary tumor, serum CEA level > 200 ng/ml. Stepwise backward regression was used to exclude variables from the model when *P*>.1. All statistical tests were two-sided and executed using IBM SPSS Statistics 20.0 software (SPSS Inc., Illinois, USA). *P* values <.05 were considered significant.

## Supplementary Material

Refer to Web version on PubMed Central for supplementary material.

## Acknowledgments

## References

1. Peroz D, Rodriguez N, Choveau F, Baro I, Merot J, Loussouarn G. Kv7. 1 (KCNQ1) properties and channelopathies. J Physiol. 2008; 586:1785–9. [PubMed: 18174212]

2. Winbo A, Sandstrom O, Palmqvist R, Rydberg A. Iron-deficiency anaemia, gastric hyperplasia, and elevated gastrin levels due to potassium channel dysfunction in the Jervell and Lange-Nielsen Syndrome. Cardiol Young. 2012; 18:1–10.

3. Grahammer F, Herling AW, Lang HJ, Schmitt-Graff A, Wittekindt OH, Nitschke R, et al. The cardiac K+ channel KCNQ1 is essential for gastric acid secretion. Gastroenterology. 2001; 120:1363–71. [PubMed: 11313306]

4. Rice KS, Dickson G, Lane M, Crawford J, Chung SK, Rees MI, et al. Elevated serum gastrin levels in Jervell and Lange-Nielsen syndrome: a marker of severe KCNQ1 dysfunction? Heart Rhythm. 2011; 8:551–4. [PubMed: 21118729]

5. Nikou GC, Toubanakis C, Moulakakis KG, Pavlatos S, Kosmidis C, Mallas E, et al. Carcinoid tumors of the duodenum and the ampulla of Vater: current diagnostic and therapeutic approach in a series of 8 patients. Case series. Int J Surg. 2011; 9:248–53. [PubMed: 21215338]

6. Unoki H, Takahashi A, Kawaguchi T, Hara K, Horikoshi M, Andersen G, et al. SNPs in KCNQ1 are associated with susceptibility to type 2 diabetes in East Asian and European populations. Nat Genet. 2008; 40:1098–102. [PubMed: 18711366]

7. Yasuda K, Miyake K, Horikawa Y, Hara K, Osawa H, Furuta H, et al. Variants in KCNQ1 are associated with susceptibility to type 2 diabetes mellitus. Nat Genet. 2008; 40:1092–7. [PubMed: 18711367]

8. Starr TK, Allaei R, Silverstein KA, Staggs RA, Sarver AL, Bergemann TL, et al. A transposon-based genetic screen in mice identifies genes altered in colorectal cancer. Science. 2009; 323:1747–50. [PubMed: 19251594]

9. March HN, Rust AG, Wright NA, ten Hoeve J, de Ridder J, Eldridge M, et al. Insertional mutagenesis identifies multiple networks of cooperating genes driving intestinal tumorigenesis. Nat Genet. 2011; 43:1202–9. [PubMed: 22057237]

10. Mann KM, Ward JM, Yew CC, Kovochich A, Dawson DW, Black MA, et al. Sleeping Beauty mutagenesis reveals cooperating mutations and pathways in pancreatic adenocarcinoma. Proc Natl Acad Sci U S A. 2012; 109:5934–41. [PubMed: 22421440]

11. Perez-Mancera PA, Rust AG, van der Weyden L, Kristiansen G, Li A, Sarver AL, et al. The deubiquitinase USP9X suppresses pancreatic ductal adenocarcinoma. Nature. 2012; 486:266–70. [PubMed: 22699621]

12. Starr TK, Scott PM, Marsh BM, Zhao L, Than BL, O'Sullivan MG, et al. A Sleeping Beauty transposon-mediated screen identifies murine susceptibility genes for adenomatous polyposis coli

(Apc)-dependent intestinal tumorigenesis. Proc Natl Acad Sci U S A. 2011; 108:5765–70. [PubMed: 21436051]

13. Lee MP, Ravenel JD, Hu RJ, Lustig LR, Tomaselli G, Berger RD, et al. Targeted disruption of the Kvlqt1 gene causes deafness and gastric hyperplasia in mice. J Clin Invest. 2000; 106:1447–55. [PubMed: 11120752]

14. Casimiro MC, Knollmann BC, Ebert SN, Vary JC Jr, Greene AE, Franz MR, et al. Targeted disruption of the Kcnq1 gene produces a mouse model of Jervell and Lange-Nielsen Syndrome. Proc Natl Acad Sci U S A. 2001; 98:2526–31. [PubMed: 11226272]

15. Casimiro MC, Knollmann BC, Yamoah EN, Nie L, Vary JC Jr, Sirenko SG, et al. Targeted point mutagenesis of mouse Kcnq1: phenotypic analysis of mice with point mutations that cause Romano-Ward syndrome in humans. Genomics. 2004; 84:555–64. [PubMed: 15498462]

16. Takagi T, Nishio H, Yagi T, Kuwahara M, Tsubone H, Tanigawa N, et al. Phenotypic analysis of vertigo 2 Jackson mice with a Kcnq1 potassium channel mutation. Exp Anim. 2007; 56:295–300. [PubMed: 17660684]

17. Elso CM, Lu X, Culiat CT, Rutledge JC, Cacheiro NL, Generoso WM, et al. Heightened susceptibility to chronic gastritis, hyperplasia and metaplasia in Kcnq1 mutant mice. Hum Mol Genet. 2004; 13:2813–21. [PubMed: 15385447]

18. Demolombe S, Franco D, de Boer P, Kuperschmidt S, Roden D, Pereon Y, et al. Differential expression of KvLQT1 and its regulator IsK in mouse epithelia. Am J Physiol Cell Physiol. 2001; 280:C359–72. [PubMed: 11208532]

19. Dedek K, Waldegger S. Colocalization of KCNQ1/KCNE channel subunits in the mouse gastrointestinal tract. Pflugers Arch. 2001; 442:896–902. [PubMed: 11680623]

20. Vallon V, Grahammer F, Volkl H, Sandu CD, Richter K, Rexhepaj R, et al. KCNQ1-dependent transport in renal and gastrointestinal epithelia. Proc Natl Acad Sci U S A. 2005; 102:17864–9. [PubMed: 16314573]

21. Warth R, Garcia Alzamora M, Kim JK, Zdebik A, Nitschke R, Bleich M, et al. The role of KCNQ1/KCNE1 K(+) channels in intestine and pancreas: lessons from the KCNE1 knockout mouse. Pflugers Arch. 2002; 443:822–8. [PubMed: 11889581]

22. Munoz J, Stange DE, Schepers AG, van de Wetering M, Koo BK, Itzkovitz S, et al. The Lgr5 intestinal stem cell signature: robust expression of proposed quiescent '+4' cell markers. EMBO J. 2012; 31:3079–91. [PubMed: 22692129]

23. IPA Ingenuity Systems. [Accessed February 2, 2013] Available at http://www.ingenuity.com

24. Subramanian A, Tamayo P, Mootha VK, et al. Gene set enrichment analysis: a knowledge-based approach for interpreting genome-wide expression profiles. Proc Natl Acad Sci U S A. 2005; 102:15545–50. [PubMed: 16199517]

25. Norkina O, Kaur S, Ziemer D, De Lisle RC. Inflammation of the cystic fibrosis mouse small intestine. Am J Physiol Gastrointest Liver Physiol. 2004 Jun; 286(6):G1032–41. Epub 2004 Jan 22. [PubMed: 14739145]

26. DeBerardinis RJ, Lum JJ, Hatzivassiliou G, Thompson CB. The biology of cancer: metabolic reprogramming fuels cell growth and proliferation. Cell Metab. 2008 Jan; 7(1):11–20.10.1016/j.cmet.2007.10.002 [PubMed: 18177721]

27. Knobloch M, Braun SM, Zurkirchen L, von Schoultz C, Zamboni N, Araúzo-Bravo MJ, et al. Metabolic control of adult neural stem cell activity by Fasn-dependent lipogenesis. Nature. 2013 Jan 10; 493(7431):226–30. Epub 2012 Dec 2. 10.1038/nature11689 [PubMed: 23201681]

28. Duerkop BA, Vaishnava S, Hooper LV. Immune responses to the microbiota at the intestinal mucosal surface. Immunity. 2009 Sep 18; 31(3):368–76.10.1016/j.immuni.2009.08.009 [PubMed: 19766080]

29. Shalapour S, Deiser K, Sercan O, Tuckermann J, Minnich K, Willimsky G, et al. Commensal microflora and interferon-gamma promote steady-state interleukin-7 production in vivo. Eur J Immunol. 2010 Sep; 40(9):2391–400.10.1002/eji.201040441 [PubMed: 20690180]

30. Vaishnava S, Yamamoto M, Severson KM, Ruhn KA, Yu X, Koren O, et al. The antibacterial lectin RegIIIgamma promotes the spatial segregation of microbiota and host in the intestine. Science. 2011 Oct 14; 334(6053):255–8.10.1126/science.1209791 [PubMed: 21998396]

31. Dziarski R, Gupta D. Review: Mammalian peptidoglycan recognition proteins (PGRPs) in innate immunity. Innate Immun. 2010 Jun; 16(3):168–74. Epub 2010 Apr 23. 10.1177/1753425910366059 [PubMed: 20418257]

32. Kang S, Okuno T, Takegahara N, Takamatsu H, Nojima S, Kimura T, et al. Intestinal epithelial cell-derived semaphorin 7A negatively regulates development of colitis via αvβ1 integrin. J Immunol. 2012 Feb 1; 188(3):1108–16. Epub 2011 Dec 23. 10.4049/jimmunol.1102084 [PubMed: 22198947]

33. Hashimoto T, Perlot T, Rehman A, Trichereau J, Ishiguro H, Paolino M, et al. ACE2 links amino acid malnutrition to microbial ecology and intestinal inflammation. Nature. 2012 Jul 25; 487(7408):477–81.10.1038/nature11228 [PubMed: 22837003]

34. Lang F, Shumilina. Regulation of ion channels by the serum- and glucocorticoid-inducible kinase SGK1. FASEB J. 2013 Jan; 27(1):3–12. Epub 2012 Sep 25. 10.1096/fj.12-218230 [PubMed: 23012321]

35. De Lisle RC, Mueller R, Boyd M. Impaired mucosal barrier function in the small intestine of the cystic fibrosis mouse. J Pediatr Gastroenterol Nutr. 2011; 53:371–9. [PubMed: 21970994]

36. Yang K, Popova NV, Yang W, Lozonschi I, Tadesse S, Kent S, et al. Interaction of *Muc2* and *Apc* on Wnt signaling and in intestinal tumorigenesis: potential role of chronic inflammation. Cancer Research. 2008; 68:7313–7322. [PubMed: 18794118]

37. Burger-van Paassen N, Loonen LM, Witte-Bouma J, Korteland-van Male AM, de Bruijn AC, van der Sluis M, et al. Mucin Muc2 deficiency and weaning influences the expression of the innate defense genes Reg3β, Reg3γ and angiogenin-4. PLoS One. 2012; 7:e38798. [PubMed: 22723890]

38. Xiong Q, Gao Z, Wang W, Li M. Activation of Kv7 (KCNQ) voltage-gated potassium channels by synthetic compounds. Trends Pharmacol Sci. 2008 Feb; 29(2):99–107. Epub 2008 Jan 18. 10.1016/j.tips.2007.11.010 [PubMed: 18206251]

39. Wulff H, Castle NA, Pardo LA. Voltage-gated potassium channels as therapeutic targets. Nat Rev Drug Discovery. 2009; 8:982–1001. [PubMed: 19949402]

40. Preston P, Wartosch L, Günzel D, Fromm M, Kongsuphol P, Ousingsawat J, Kunzelmann K, Barhanin J, Warth R, Jentsch TJ. Disruption of the K+ channel beta-subunit KCNE3 reveals an important role in intestinal and tracheal Cl- transport. J Biol Chem. 2010; 285:7165–75.10.1074/jbc.M109.047829 [PubMed: 20051516]

41. Maisonneuve P, FitzSimmons SC, Neglia JP, Campbell PW 3rd, Lowenfels AB. Cancer risk in nontransplanted and transplanted cystic fibrosis patients: a 10-year study. J Natl Cancer Inst. 2003; 95:381–7. [PubMed: 12618503]

42. Fijneman RJA, Anderson R, Richards E, Liu J, Tijssen M, Meijer GA, et al. *Runx1* is a tumor suppressor gene in the mouse gastrointestinal tract. Cancer Science. 2012; 103:593–92011. [PubMed: 22171576]

43. Sato T, Stange DE, Ferrante M, Vries RG, Van Es JH, Van den Brink S, et al. Long-term expansion of epithelial organoids from human colon, adenoma, adenocarcinoma, and Barrett's epithelium. Gastroenterology. Nov.141:1762–72. [PubMed: 21889923]

44. Mootha VK, Lindgren CM, Eriksson KF, et al. PGC-1alpha-responsive genes involved in oxidative phosphorylation are coordinately downregulated in human diabetes. Nat Genet. 2003; 34:267–73. [PubMed: 12808457]

45. Rotterdam, Stichting FMWV. Code Goed Gebruik van lichaamsmateriaal. 2011.

46. Simon R, Mirlacher M, Sauter G. Tissue microarrays. Biotechniques. 2004; 36:98–105. [PubMed: 14740491]

47. Belt EJT, Fijneman RJA, van den Berg EG, et al. Loss of lamin A/C expression in stage II and III colon cancer is associated with disease recurrence. Eur J Cancer. 2011; 47:1837–1845. [PubMed: 21621406]

48. Zlobec I, Steele R, Terracciano L, et al. Selecting immunohistochemical cutoff scores for novel biomarkers of progression and survival in colorectal cancer. J Clin Pathol. 2007; 60:1112–1116. [PubMed: 17182662]

49. Fong Y, Fortner J, Sun RL, et al. Clinical score for predicting recurrence after hepatic resection for metastatic colorectal cancer: analysis of 1001 consecutive cases. Ann Surg. 1999; 230:309–318. [PubMed: 10493478]
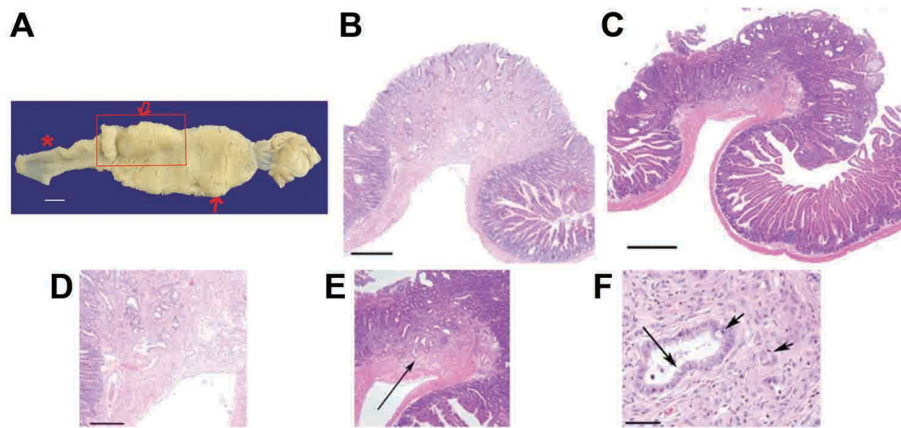
**Figure 1. Loss of *Kcnq1* promotes tumor progression**

Panel 1A. Duodenum from $Apc^{Min} Kcnq1^{+/-}$ mouse with stomach at right. Bar = 5 mm. Broad area of hyperplastic tissue with embedded tumors extends from pylorus-dudoenum juncture past the ampulla to ~ the duodenal jejunal flexure. Asterisk indicates area of normal duodenum-proximal jejunum. Box encloses a region of adenocarcinoma tissue of > 2 cm. Sections from this lesion were taken from various regions and all showed evidence of invasion. Two of these adenocarcinoma sections are depicted in panels B through E. Smaller arrow depicts normal large adenoma of ~ 5 mm that is embedded in hyperplastic tissue. Panels B&C, bars = 500 μm; invasion into muscularis mucosa, panels D&E, bar = 250 μm; prominent scirrhous response to invading tubules that exhibit differentiated goblet cells (long arrow) and signet ring cells (short arrows) panel E, bar = 50 μm.
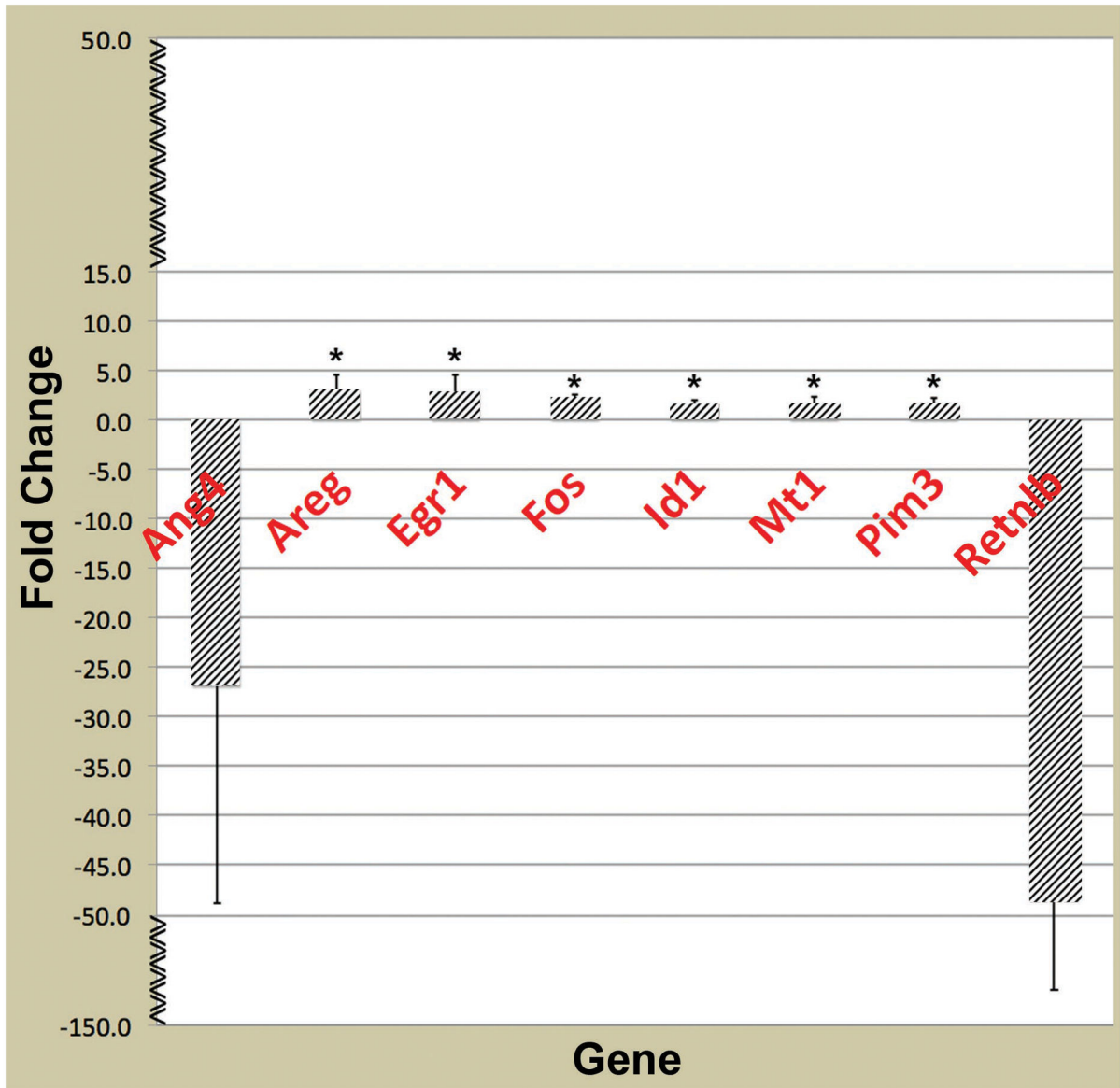
**Figure 2. qRT-PCR gene expression analysis of mouse colon**

Samples were analyzed in triplicate and normalized to 18S ribosomal RNA. Data are presented as the mean fold change +/− SD. Each bar represents the mean and standard error of multiple experiments that measured fold differences in the mRNA expression of whole colon tissue isolated from adult (~ 100 d), littermate and gender matched pairs of $Apc^{+/+}$ $Kcnq1^{-/-}$ and $Kcnq1^{+/+}$ mice. RNA was isolated from 1 cm sections from the same region of distal colon. At least two matched pairs of mRNAs were tested for each gene with most genes tested in at least three matched pairs of mRNAs. To be included in this figure genes showed a mean fold difference of at least 1.5. In all cases the direction in changes in gene expression confirmed microarray data. * P<0.05.
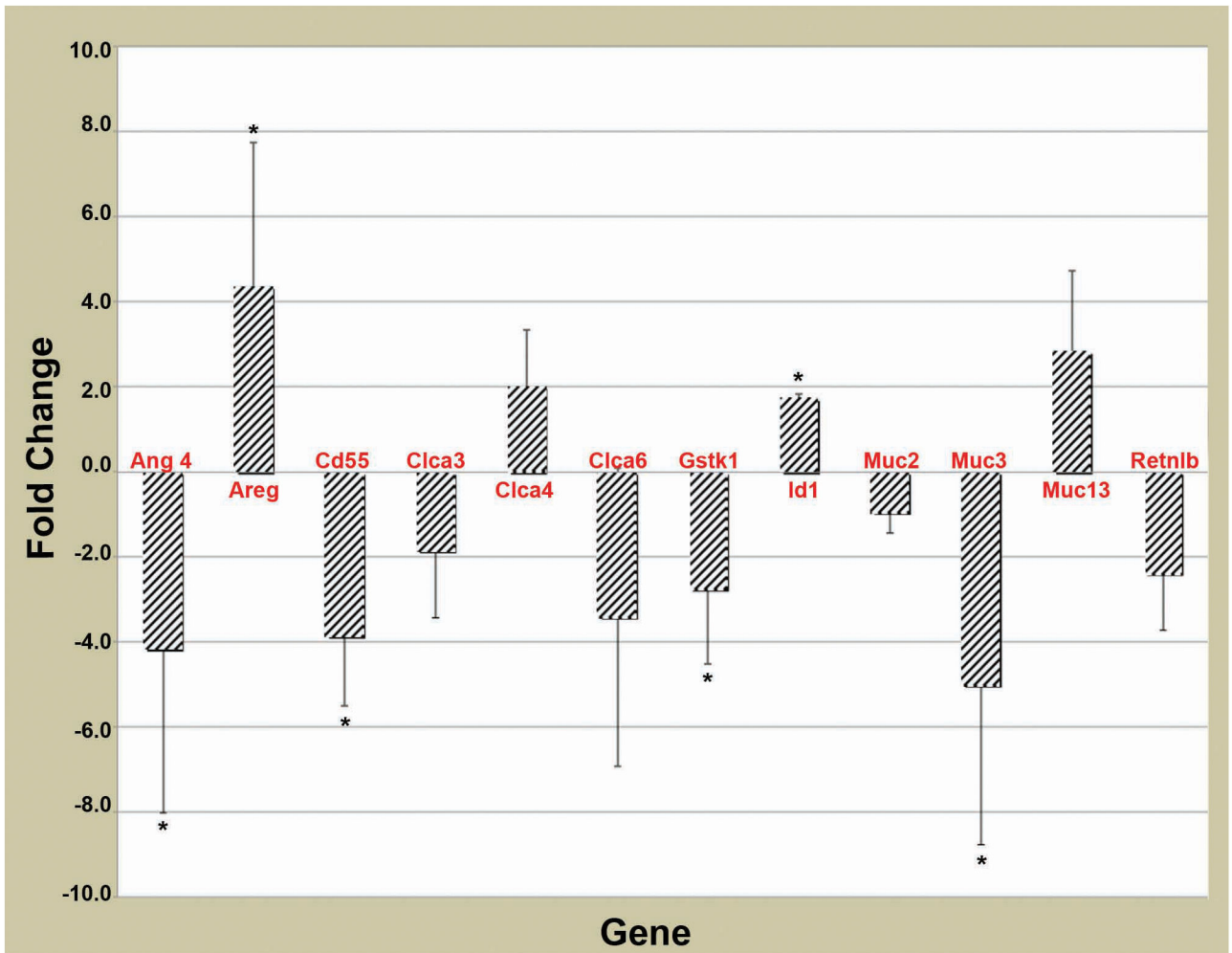
**Figure 3. qRT-PCR gene expression analysis of mouse proximal small intestine**
Each gene sample was run in triplicate and gene expression was normalized to the expression of 18S. Data are presented as the mean fold change +/− SD. Each bar represents the mean and standard error of multiple experiments that measured fold differences in the mRNA expression in proximal small intestine tissue isolated from adult (~100 d) littermate and gender matched pairs of $Apc^{+/+}$ $Kcnq1^{-/-}$ and $Kcnq1^{+/+}$ mice. mRNAs were isolated from 1 cm sections of proximal small intestine from the same region for all mice. At least two matched pairs of mRNAs were tested for each gene with most genes tested in at least three matched pairs of mRNAs. To be included in this figure genes showed a mean fold difference was at least 1.5. In all cases the direction of changes in gene expression confirmed microarray data. * P<0.05.
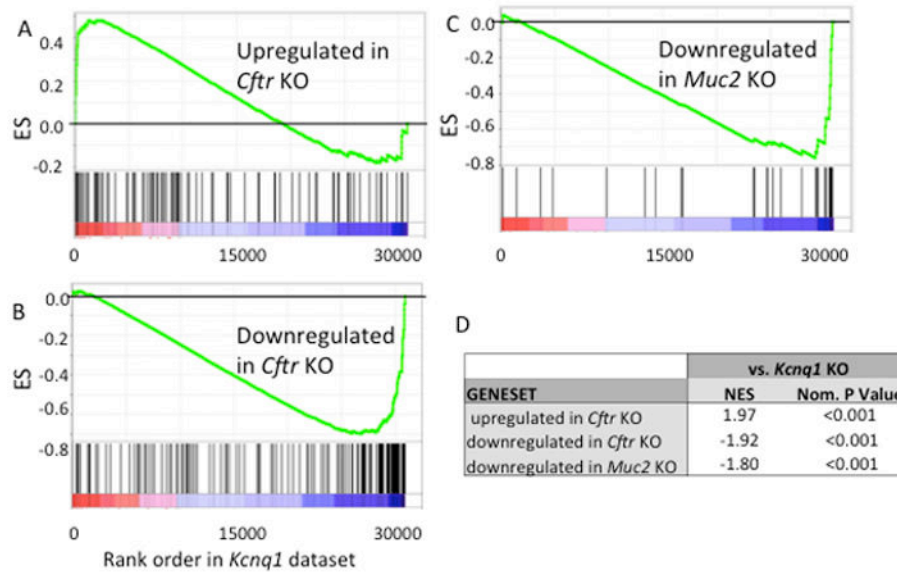
**Figure 4. GSEA**
Results of GSEA showing enrichment scores (ES) of *Cftr* and *Muc2* genesets with respect to the ranked *Kcnq1* expression dataset. Shown are enrichment plots for genesets consisting of (A) genes upregulated in the small intestine of CFTR KO mice[27]; (B) genes downregulated in the small intestine of CFTR KO mice[27];(C) genes downregulated in the small intestine of *Muc2* KO mice[37]. (D) Normalized enrichment score (NES) and nominal P value (nom. P value) are shown for each comparison.
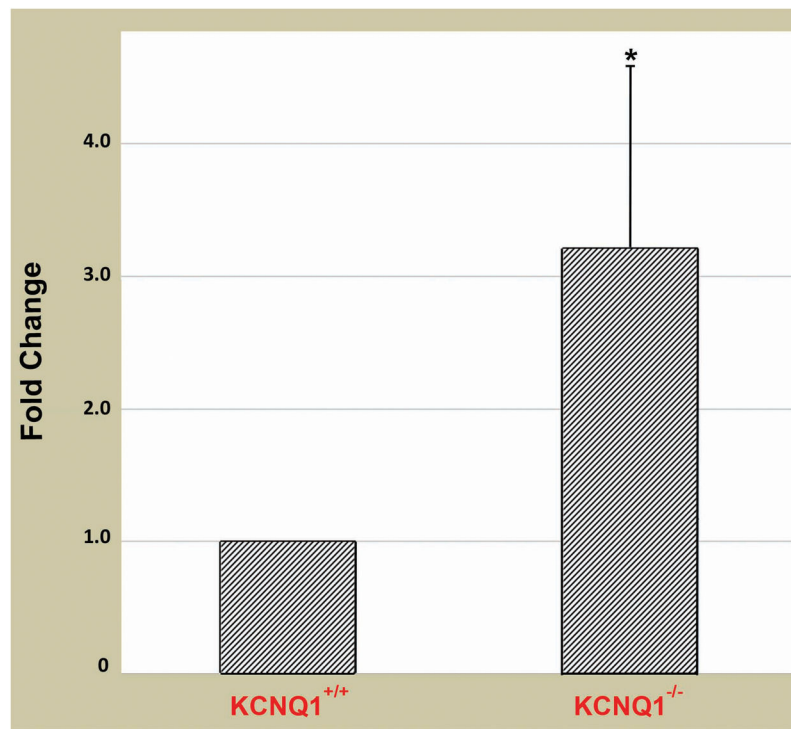
**Figure 5. Colon Organoids**

Colon organoids were created from 500 crypt bottoms and plated in triplicate in 24-well plates. Crypt bottoms were isolated on separate days from 5 of each, age, gender and littermate matched $Apc^{+/+} Kcnq1^{-/-}$ and $Apc^{+/+} Kcnq1^{+/+}$ mice (one matched pair per day). Organoids were examined daily and counted at 5 days post-plating. * P <0.05.
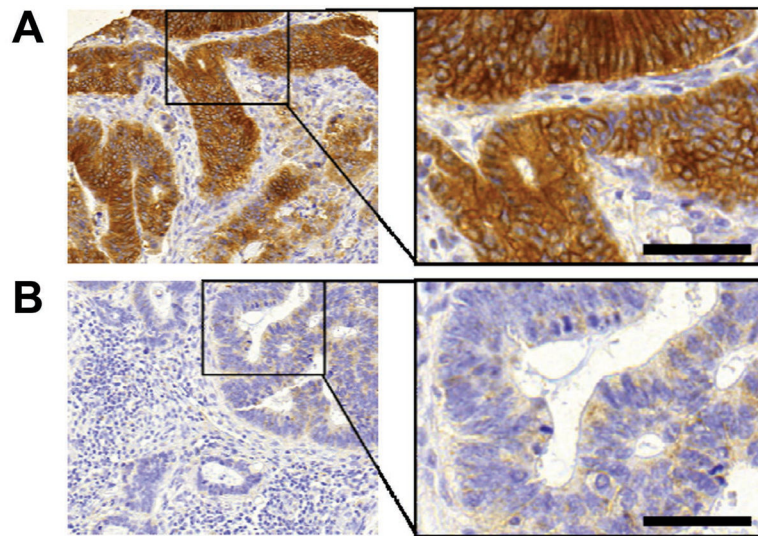
**Figure 6. Representative human samples showing the expression pattern of KCNQ1 in epithelium of CRCLM**

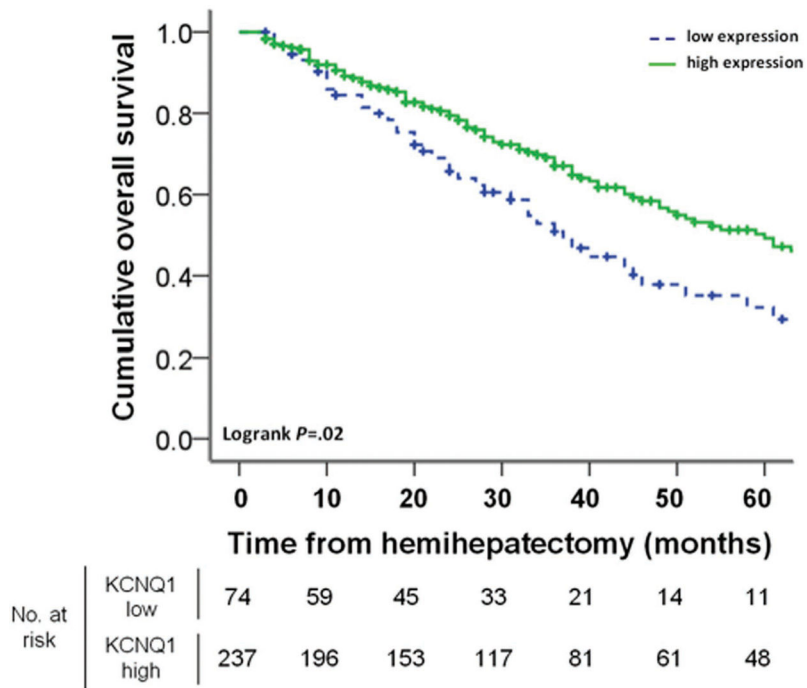Staining intensity was evaluated as (A) high or (B) low. Scale bars are 50 μm.

**Figure 7. Kaplan-Meier graph depicting OS in months, stratified by intensity of KCNQ1 expression in CRCLMs**

P-values were calculated using the logrank statistic.

**Table 1**

Loss of *Kcnq1* enhances tumor multiplicity in *Apc^Min* mice.

| Males | N | colon | Proximal SI | Distal SI |
|---|---|---|---|---|
| *Kcnq1* ^+/+ | 30 | 1.8 ± 1.7 | 11 ± 8 | 56 ± 41 |
| *Kcnq1* ^+/− | 34 | *3.8 ± 2.3 | *18 ± 13 | *76 ± 38 |
| *Kcnq1* ^−/− | 10 | 2.6 ± 2.8 | *36 ± 16 | 52 ± 43 |
| Females | | | | |
| *Kcnq1* ^+/+ | 26 | 1.2 ± 1.7 | 14 ± 9 | *58 ± 25 |
| *Kcnq1* ^+/− | 46 | *2.5 ± 2.2 | 20 ± 12 | *84 ± 37 |
| *Kcnq1* ^−/− | 13 | 2.1 ± 2.0 | *22 ± 11 | 30 ± 16 |

$Apc^{Min}$ $Kcnq1^{+/+}$, $Apc^{Min}$ $Kcnq1^{+/-}$ and $Apc^{Min}Kcnq1^{-/-}$ mice were sacrificed at 120 days of age and tumors counted and measured.

*
P values: < 0.05; Two-sided P values for tumor counts were determined by use of the Wilcoxon Rank Sum Test comparing gender and age-matched classes produced in the same genetic crosses.

**Table 2**

*Apc^Min Kcnq1^−/−* tumor phenotype is strongest in the proximal quarter of the small intestine.

| Males | tumors | Females | tumors |
|---|---|---|---|
| *Kcnq1* ^+/+ | 4 ± 2 | *Kcnq1* ^+/+ | 5 ± 3 |
| *Kcnq1* ^+/− | 6 ± 3 | *Kcnq1* ^+/− | 8 ± 4 |
| *Kcnq1* ^−/− | *21 ± 11 | *Kcnq1* ^−/− | *15 ± 9 |

Mice and tissues are the same as Table 1.

*
 P values: < 0.05; Two-sided P values for tumor counts were determined by use of the Wilcoxon Rank Sum Test comparing gender and age-matched classes produced in the same genetic crosses.